Selective crystallization of calcium salts by poly(acrylate)-grafted chitosan

Andrónico Neira-Carrillo [a,b,c], Mehrdad Yazdani-Pedram [c,d], Jaime Retuert [b,c], Mario Diaz-Dosque [c,e], Sebastien Gallois [b], José L. Arias [a,c,*]

[a] *Faculty of Veterinary and Animal Sciences, University of Chile, Santiago, Chile*
[b] *Faculty of Physics and Mathematics, University of Chile, Santiago, Chile*
[c] *Center for Advanced Interdisciplinary Research in Materials (CIMAT), Santiago, Chile*
[d] *Faculty of Chemistry and Pharmacy, University of Chile, Santiago, Chile*
[e] *Faculty of Odontology, University of Chile, Santiago, Chile*

Abstract

The biopolymer chitosan was chemically modified by grafting polyacrylamide or polyacrylic acid in a homogeneous aqueous phase using potassium persulfate (KPS) as redox initiator system in the presence of *N*,*N*-methylene-bis-acrylamide as a crosslinking agent. The influence of the grafted chitosan on calcium salts crystallization in vitro was studied using the sitting-drop method. By using polyacrylamide grafted chitosan as substrate, rosette-like $CaSO_4$ crystals were observed. This was originated by the presence of sulfate coming from the initiator KPS. By comparing crystallization on pure chitosan and on grafted chitosan, a dramatic influence of the grafted polymer on the crystalline habit of both salts was observed. Substrates prepared by combining sulfate with chitosan or sulfate with polyacrylamide did not produce similar $CaSO_4$ morphologies. Moreover, small spheres or donut-shaped $CaCO_3$ crystals on polyacrylic acid grafted chitosan were generated. The particular morphology of $CaCO_3$ crystals depends also on other synthetic parameters such as the molecular weight of the chitosan sample and the KPS concentration.

Keywords: Chitosan; Crystallization; Calcium carbonate; Calcium sulfate; Polymorphs

1. Introduction

In nature, biological organisms produce organo-inorganic polymeric hybrids as functional structural materials (eggshells, seashells, and bone) [1]. Small amounts of acid-rich proteins and proteoglycans play a major role in forming these hybrids by influencing mineral crystal nucleation and growth [2–5]. Calcium carbonate is the major inorganic material in these systems, but biogenic $CaSO_4$ also occurs [6]. Calcium carbonate has three polymorph: calcite (hexagonal), aragonite (orthorhombic), and vaterite (hexagonal). On the other hand, the calcium sulfate–H_2O system is characterized by different solid phases, which are differentiated by their degree of hydration: $CaSO_4{\cdot}2H_2O$ (calcium sulfate dihydrate or gypsum), $CaSO_4{\cdot}(1/2)H_2O$ (calcium sulfate hemihydrate), and $CaSO_4$ (calcium sulfate anhydrite) [7]. Therefore, understanding the mechanism of growth and inhibition during crystallization of calcium sulfate and calcium carbonate is of primary importance for biomedical and industrial applications. An important factor for successfully coating an organic polymer substrate with crystals is to increase the charge density or polarity and solubility on the surface of the polymer.

In this case, we have used flakes of chitosan (CHI) chemically modified by grafting as crystallization substrate. The CHI (poly-β-(1→4)-2-amino-2-deoxy-D-glucose) is obtained through partial deacetylation of chitin (poly-β(1→4)-

* Corresponding author. Fax: +56(2)5416840.
E-mail address: jarias@uchile.cl (J.L. Arias).

2-acetamido-2-deoxy-D-glucose), which is the second most abundant polysaccharide in nature. Although most of the work on crystallization of these salts has been done in solution, only a few investigations have been carried out on the surfaces of films or gels [8–17]. Generally, the biopolymers chitin and chitosan are insoluble and do not form film materials. However, when grafted with poly(acrylic acid) or polyacrylamide, they become insoluble, are able to form flakes with a nearly flat surface, and show functional groups that can influence crystal nucleation and growth [18–22]. To our best knowledge, the spatial distribution of polar functional groups, that is, the local charge density, is of crucial importance for the nucleation and determines the orientation of crystals. The importance of the nonspecific electrostatic effects such as charge density has been determined previously by Volkmer et al. [23].

Therefore, it is interesting to study the effect of these grafted chains on the crystalline habit of calcium salts. Here we report the preparation of these grafted polymers and their application as substrates for crystallization of calcium salts. The effect of these grafted chitosan matrix on the calcium salts crystallization is analyzed and compared to the crystallization within an unmodified chitosan and polyacrylamide gel as a control.

2. Materials and methods

2.1. Materials

Chitosan (CHI) samples of high molecular weight (Mw = 350 KDa, >83% deacetylation) from Aldrich and low molecular weight (Mw = 70 KDa, >75% deacetylation) from Fluka were washed with acetone and methanol and dried to constant weight. Acrylamide and acrylic acid from Aldrich, potassium persulfate (KPS) of analytical grade from BDH Chemicals, and N,N-methylene-bis-acrylamide (N,N-bis-AAM) from Fluka were used as received. Calcium chloride dihydrate, ethanol, and tris(hydroxymethyl)aminomethane were obtained from ACS-Merck and ammonium hydrogen carbonate was from J.T. Baker. These reagents were of the highest available grade and used without further purification.

2.2. Measurements

Fourier transform infrared spectra (FTIR) were obtained on a Bruker Vector 22 instrument. The samples were prepared as potassium bromide pellets. The crystals were observed in a Tesla BS 343 A scanning electron microscope (SEM). The diffraction spectrum was taken from a powdered sample using a Siemens D-5000 X-ray diffractometer with CuK_α radiation. The elemental analysis of grafted chitosan films was carried out by using an EAGER 200 (method SSabr02.EAD).

2.3. Graft copolymerization

The biopolymer chitosan was chemically modified by grafting with polyacrylamide or polyacrylic acid in a homogeneous aqueous phase by using potassium persulfate as a redox initiator in the presence of N,N-methylene-bis-acrylamide as a crosslinking agent.

Grafting reactions were carried out in 100 ml polymerization flasks by first dissolving 1 g of CHI in 40 ml of 2% acetic acid followed by the addition of monomer solution (3.3 g of acrylic acid in 40 ml of 2% acetic acid and/or 2.4 g of acrylamide in 40 ml of 2% acetic acid). The concentration of N,N-methylene-bis-acrylamide was 0.25 wt% respect to the weight of the monomers used. Two KPS concentrations of 1×10^{-2} and 2×10^{-2} M were used. The polymerization flask was closed and placed in a thermostated bath at 60 °C for 1 h. The reaction product was precipitated in acetone. The precipitate was filtered and then dried under reduced pressure to constant weight. The grafted chitosan samples were purified by exhaustive extraction with water for 24 h in order to remove the homopolymer formed during the grafting reaction and the nonreacted monomer [22]. After drying under reduced pressure the remaining product was considered to be a graft copolymer. Evidence of grafting was obtained from comparison of IR of the grafted and nongrafted chitosan.

2.4. Grafting parameters

The percentage of grafting (%G) and grafting efficiency (%E) was calculated from the increase in weight of the original CHI after grafting and extraction as follows [20–22],

$$\%G = \frac{w_2 - w_1}{w_1} \times 100, \tag{1}$$

$$\%E = \frac{w_2 - w_1}{w_3} \times 100, \tag{2}$$

where w_2, w_1 and w_3 represents the weights of grafted chitosan after extraction, initial chitosan, and monomer, respectively.

An estimation of the average degree of polymerization of grafted polyacrylic acid and/or polyacrylamide (R) was calculated by using the equation

$$R = \frac{(w_2 - w_1)M_{\mathrm{CHI}}}{M_{\mathrm{m}} w_1}, \tag{3}$$

where M_{CHI} and M_{m} represent the molar mass of the chitosan monomer unit and the molar mass of grafted vinyl monomer respectively. The R values are only approximate values since the chitosan used in this study was not 100% deacetylated, i.e., has a degree of deacetylation of 83%.

2.5. Crystallization method

Crystallization experiments were carried out in the presence of grafted chitosan samples as structure-directing substrates using the sitting-drop method [24,25] (Fig. 1). The

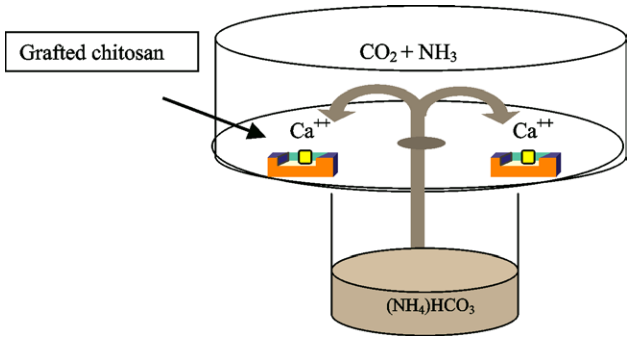

Fig. 1. Experimental setup used for growing $CaCO_3$ crystals in vitro. The concentration of $CaCl_2$ (microbridge) and of ammonium bicarbonate was 200 and 25 mM, respectively.

crystallization experiments were done using a chamber, consisting of an 85-mm plastic Petri dish having a central hole in its bottom, glued to a plastic cylindrical vessel. Inside the chamber, 3–7 mg of chitosan or chitosan-grafted flakes were put into a polystyrene microbridge. Thereafter it was filled with 35 μl of 200 mM $CaCl_2$ solution in 200 mM TRIS buffer pH 9. The cylindrical vessel contained 3 ml of 25 mM $(NH_4)HCO_3$ solution. All experiments were carried out inside the Petri dish at pH 9.0 and 20 °C for 24 h. Precipitation of $CaCO_3$ results from the diffusion of carbon dioxide (CO_2) vapor into the buffered $CaCl_2$ solution. The polymeric substrates with the crystals of the different polymorphs of $CaCO_3$ and/or $CaSO_4$ crystals formed were collected. Once rinsed with distilled water and on 50–100% gradient ethanol solutions, they were dried at room temperature and finally coated with gold using an EMS-550 automated sputter coater and analyzed by SEM.

3. Results and discussion

The mineralization of $CaCO_3$ and $CaSO_4$ using the sitting-drop method, in the presence of different grafting chitosan films, resulted in particles with different crystal structures and morphologies. The grafting of chitosans, used as templates for crystallization studies, was carried out according to the following synthetic route (Fig. 2).

Table 1
Grafting conditions and parameters for grafting of acrylamide onto chitosan (CHI-g-PAAM)

	LMW chitosan		HMW chitosan	
Chitosan[a]	1.0 g	1.0 g	1.0 g	1.0 g
KPS	1×10^{-2} M	2×10^{-2} M	1×10^{-2} M	2×10^{-2} M
AAM	2.4 g	2.4 g	2.4 g	2.4 g
Crosslinker (N,N-bis-AAM)	0.006 g	0.006 g	0.006 g	0.006 g
%G	129	125	127	73
%E	53.8	52.1	52.9	30.6
R	2.9	2.8	2.9	1.7

[a] Total volume of aqueous phase = 80 ml of 2% acetic acid.

Table 2
Grafting conditions parameters for grafting of acrylic acid onto chitosan (CHI-g-PAA)

	LMW chitosan		HMW chitosan	
Chitosan[a]	1.0 g	1.0 g	1.0 g	1.0 g
KPS	1×10^{-2} M	2×10^{-2} M	1×10^{-2} M	2×10^{-2} M
AA	3.330 g	3.330 g	3.330 g	3.330 g
Crosslinker (N,N-bis-AAM)	0.008 g	0.008 g	0.008 g	0.008 g
%G	205	179	266	244
%E	61.4	53.7	79.9	73.4
R	4.6	4.0	6.0	5.5

[a] Total volume of aqueous phase = 80 ml of 2% acetic acid.

Tables 1 and 2 show the percentage of grafting (%G), grafting efficiency (%E), and the length of the grafted chains (R) for the optimized grafting reactions of acrylamide and acrylic acid onto chitosan, respectively [20].

It can be seen from Tables 1 and 2 that higher %E is obtained for a KPS concentration of 1×10^{-2} M for both systems CHI-g-PAA and CHI-g-PAAM when low-molecular-weight chitosan was used. In the CHI-g-PAAM system, the %E was slightly lower, probably due to the consumption of monomer to form homopolymer. This favors the possible combination of the chitosan macroradicals with the existing excess of primary free radicals present in the reaction medium. The homopolymer formation and grafted polyacrylamide chains could be crucial for the interaction with sulfate groups coming from KPS and allowed the $CaSO_4$ crystals (gypsum) formation in this system. The presence

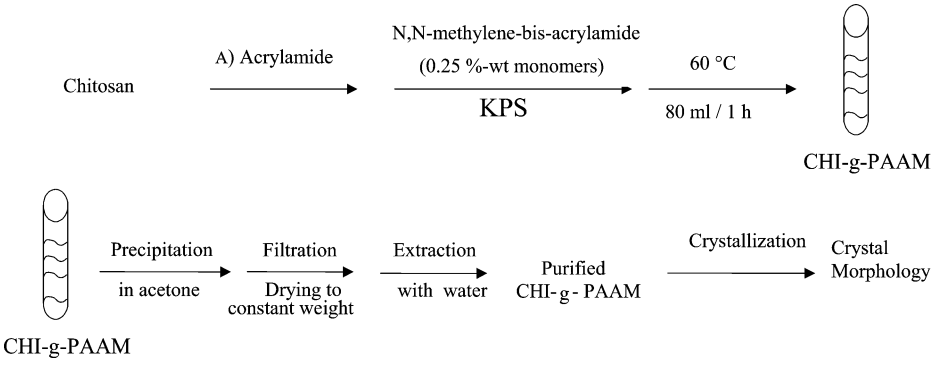

Fig. 2. Synthetic route for obtaining CHI-g-PAAM grafted chitosan. The same procedure was used for CHI-g-PAA.

Table 3
Elemental analysis of CHI-g-PAAM and CHI-g-PAA films

Sample	[KPS] (M)	%N	%C	%H	%S
CHI-g-PAAM (from LMW)	2×10^{-2}	13.8	41.2	7.9	1.2
CHI-g-PAAM (from HMW)	1×10^{-2}	12.2	39.7	7.4	1.5
CHI-g-PAA (from HMW)	1×10^{-2}	1.88	47.6	6.6	0.0
CHI-g-PAA (from LMW)	2×10^{-2}	1.68	46.8	6.3	0.0

of sulfur (Table 3) and the sulfate groups (Fig. 3) were confirmed by elemental analysis and FTIR spectroscopy, respectively. In the case of CHI-g-PAA system, the highest $\%E$ was found by using high molecular weight chitosan at 1×10^{-2} M concentration.

The IR spectrum of the grafted chitosan is in agreement with the proposed molecular structure. Infrared spectra from grafted chitosan and chitosan of high and low molecular weights are shown in Figs. 3A and 3B. The comparison of IR spectra of chitosan and grafted chitosan show that effectively the grafting has taken place. The absorption band at 3429 cm^{-1} is due to NH bonds of chitosan (Fig. 3A1 and 3B1) and those at 1564 and 1651 cm^{-1} correspond to amide I and II bands respectively.

On the other hand, the spectrum of chitosan grafted with polyacrylamide (PAAM) (Fig. 3A2) shows a strong absorption band at 1673 cm^{-1} corresponding to amine–carbonyl absorption from PAAM chains. In polyacrylamide homopolymer this band is located at 1670 cm^{-1}. The most typical absorption bands of chitosan corresponding to amide I and II bands, are not clearly visible in the grafted product since they are hidden by a strong and broad carbonyl absorption band of PAAM in this spectral region. However, the chitosan amide I absorption band could be observed as a shoulder at 1602 cm^{-1}. The shift of the carbonyl absorption band of PAAM grafted chitosan (CHI-g-PAAM) to lower frequencies could be due to the inter-and/or intramolecular interactions through hydrogen bonding (Figs. 3A2 and 3B2). Both spectra for PAAM grafted chitosan show two new absorption bands at 1322 and 1087 cm^{-1} attributed to the presence of sulfate groups coming from the initiator (KPS) [26,27].

The sulfate contained in the CHI-g-PAAM, in spite of the exhaustive extraction process with water, explains the presence of calcium sulfate crystals when this product was used as a substrate for crystallization. For chitosan grafted with polyacrylic acid (PAA) an absorption band at 1732 and at 1735 cm^{-1} were assigned to the carbonyl groups from poly(acrylic acid)-grafted chitosan of high and low molecular weight, respectively [22]. Both chitosan samples grafted with poly(acrylic acid) (CHI-g-PAA) also showed an absorption band at 1627 cm^{-1} corresponding to the amide group (Figs. 3A3 and 3B3).

Table 3 shows the elemental analysis of CHI-g-PAAM and CHI-g-PAA. The results are in agreement with the presence and absence of the sulfate groups in CHI-g-PAAM and CHI-g-PAA, respectively, as was previously observed in the IR analysis (Fig. 3). The absence of sulfur in the CHI-g-PAA material indicates that charged PAA chains are not able to coordinate sulfate ions at difference of PAAM grafted chitosan. The carbon and hydrogen relative contents of CHI-g-PAAM and CHI-g-PAA products are similar and independent of the molecular weight of the ungrafted chitosan. As expected, the CHI-g-PAAM has higher nitrogen content that CHI-g-PAA.

The influence of the grafted chitosan films on the $CaCO_3$ and $CaSO_4$ crystallization in vitro was studied using the sitting-drop method (Fig. 4). Different Ca salts and morphologies were obtained (Table 4). Fig. 4a shows the control experiment carried out by using non-grafted CHI where calcite crystals were obtained. Fig. 4b shows the morphology

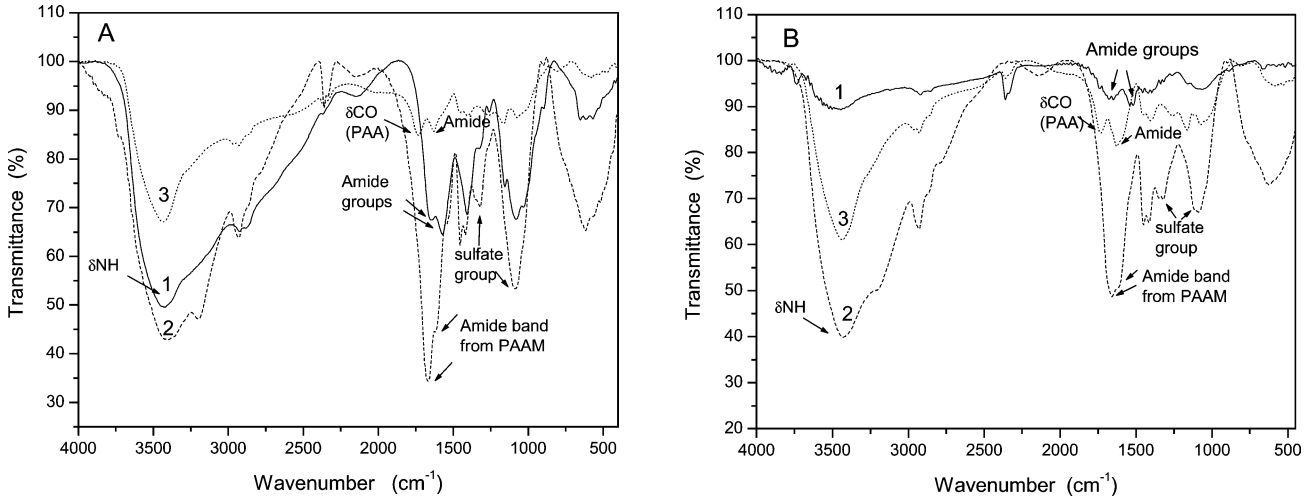

Fig. 3. FTIR spectra for the chitosan and grafted chitosan. (A1) HMW chitosan; (A2) CHI-g-PAAM; (A3) CH-g-PAA; (B1) LMW chitosan; (B2) CHI-g-PAAM; (B3) CH-g-PAA.

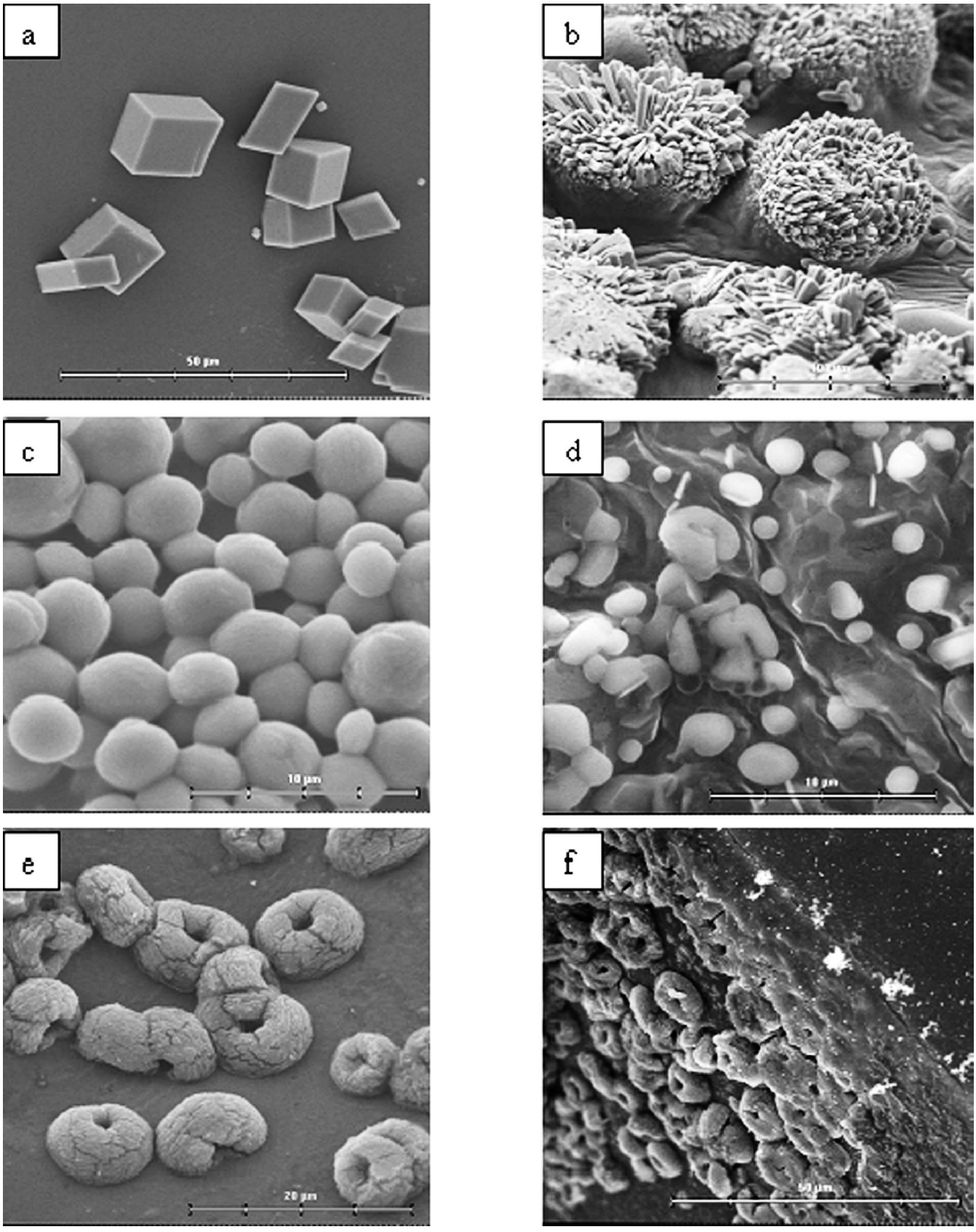

Fig. 4. SEM pictures of crystals grown in the presence of chitosan and grafted chitosan samples. (a) Chitosan control, (b) CHI-g-PAAM (HMW, KPS 1×10^{-2} M), (c) CHI-g-PAAM (LMW, KPS 2×10^{-2} M), (d) CHI-g-PAA (HMW, KPS 1×10^{-2} M), (e, f) CHI-g-PAA (LMW, KPS 1×10^{-2} M).

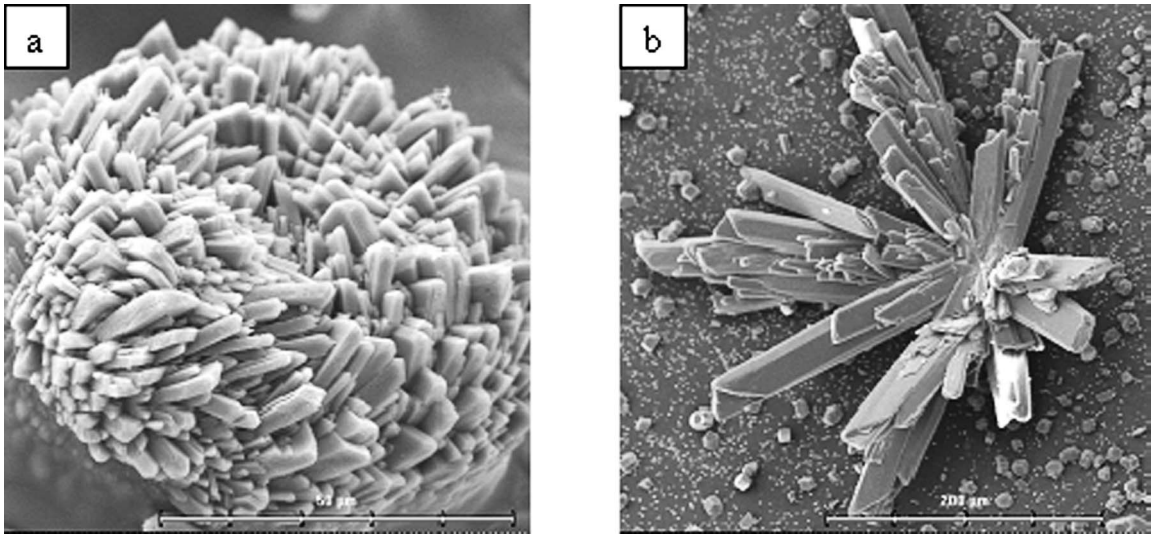

Fig. 5. SEM pictures of crystals grown in the presence of grafted chitosan samples. (a) CHI-g-PAAM (HMW, KPS 1×10^{-2} M); (b) KPS-$CaCl_2$, KPS 2×10^{-2} M, without CO_2 source.

Table 4
Crystallization in the presence of different grafted chitosan films

Sample	[KPS] (M)	Calcium salts	Morphology
CHI-g-PAAM (from HMW CHI)	1×10^{-2}	$CaSO_4$	Rosette
	2×10^{-2}	$CaSO_4$	Rosette
CHI-g-PAAM (from LMW CHI)	1×10^{-2}	$CaCO_3$	Irregular spheres
	2×10^{-2}	$CaSO_4/CaCO_3$	Rosette/spheres
CHI-g-PAA (from HMW CHI)	1×10^{-2}	$CaCO_3$	Small irregular spheres
	2×10^{-2}	$CaCO_3$	Small irregular spheres
CHI-g-PAA (from LMW CHI)	1×10^{-2}	$CaCO_3$	Donuts
	2×10^{-2}	$CaCO_3$	Donuts

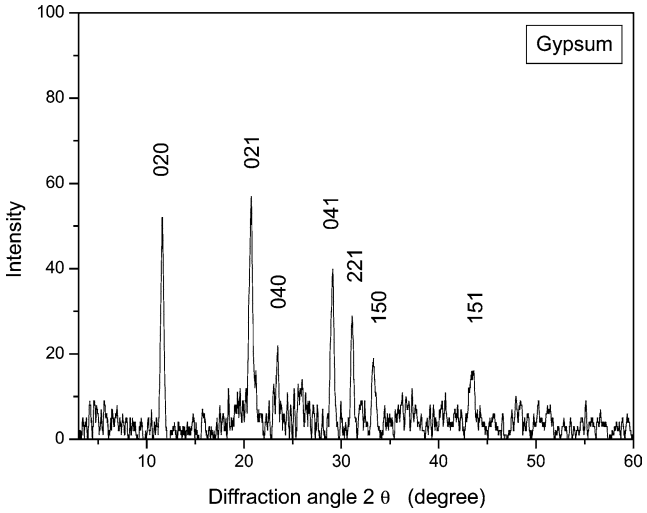

Fig. 6. XRD patterns of the calcium sulfate crystals grown on grafted chitosan samples. CHI-g-PAAM (HMW, KPS 2×10^{-2} M).

of the $CaSO_4$ rosette-like crystals obtained on CHI-g-PAAM (HMW, KPS 1×10^{-2} M), these crystals were obtained in very regular shape and size. $CaSO_4$ crystals are about 50 μm in size. Although $CaCO_3$ has a lower solubility product than $CaSO_4$, sulfate crystals are observed even after the presence of CO_2 when high molecular weight CHI is used as substrate. In fact experiments carried out in the absence of CO_2 source showed the presence of $CaSO_4$ with similar morphology as those observed in Figs. 4b and 5a. However, by using substrates obtained with low molecular weight CHI, $CaCO_3$ crystals are also formed. This could be rationalized in terms of diffusion kinetics because all the Ca is initially in sulfate form; consequently CO_2 diffuses hardly into a compact structure formed by the long chitosan chains. In contrast, the low-molecular-weight chitosan chains are less entangled, therefore the diffusion of CO_2 is facilitated, allowing the formation of $CaCO_3$ crystals.

The $CaSO_4$ precipitate of Fig. 4b was found to be calcium sulfate dihydrate or gypsum as confirmed by XRD analysis (Fig. 6). Fig. 4c shows regular spherical $CaCO_3$ crystals obtained on CHI-g-PAAM substrate (LMW, KPS 2×10^{-2} M) and Fig. 4d on CHI-g-PAA (HMW, KPS 1×10^{-2} M) substrate, respectively. Figs. 4e and 4f show the morphology of the $CaCO_3$ doughnut-like crystals obtained on CHI-g-PAA (LMW, KPS 1×10^{-2} M). Doughnut-like crystals appeared on the surface and inside the chitosan film and were between 5–10 μm in size. Fig. 4f shows transversal section of the grafted chitosan, where donut-shaped crystals were both on the surface and inside the chitosan film. Fig. 5 allows the comparison of the calcium sulfate crystal forms obtained in the presence of CHI-g-PAAM (HMW, KPS 1×10^{-2} M) and, in a control experiment, using potassium persulfate as a sulfate source dissolved in a $CaCl_2$ solution without CO_2 source as a $CaSO_4$ crystallization system at 20 °C. It can be seen that by using the grafted chitosan as substrate, very well defined rosette-like crystals of $CaSO_4$ were formed. On the other hand, in the absence of the substrate, by us-

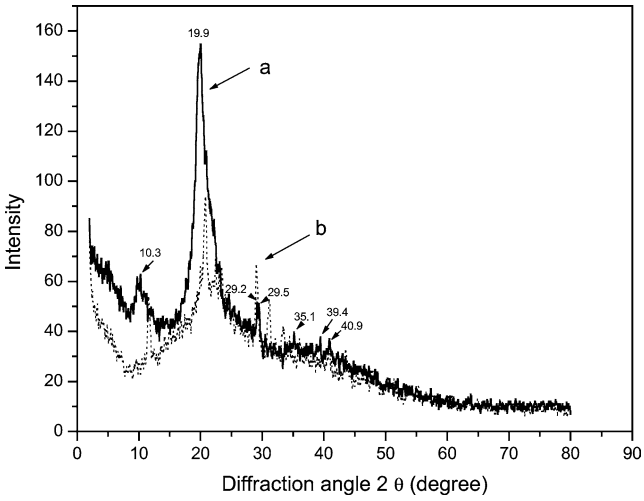

Fig. 7. XRD patterns of the calcium sulfate crystals grown on grafted chitosan samples. (a) HMW chitosan and (b) CHI-g-PAAM (HMW, KPS 1×10^{-2} M) after crystallization.

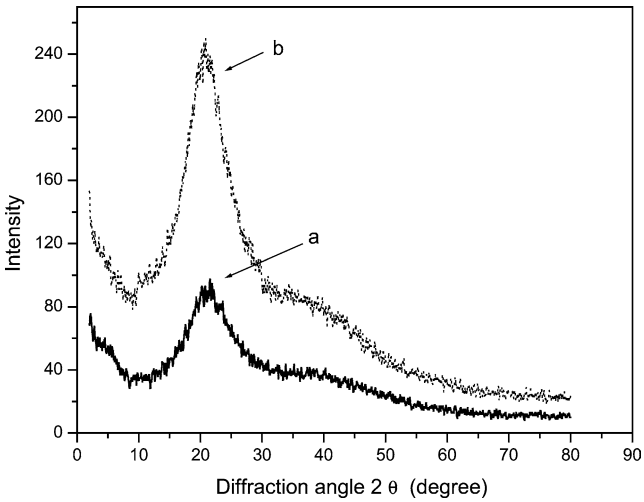

Fig. 8. XRD patterns of the calcium carbonate crystals grown on grafted chitosan samples. (a) LMW chitosan and (b) CHI-g-PAA (LMW, KPS 1×10^{-2} M) after crystallization.

ing KPS as donor of sulfate groups, irregular $CaSO_4$ crystals were formed (Fig. 5b). We can clearly see how the surface-modified substrate modulated the shape of $CaSO_4$ crystals.

Powder X-ray diffraction is a more suitable technique than electron microscopy for solids identification, and as such it was used in our crystallization assays to confirm the electron microscopic results. Fig. 7a shows the XRD patterns of the chitosan (HMW) and Fig. 7b the XRD patterns of crystals grown on the grafted CHI-g-PAAM (HMW, KPS 1×10^{-2} M). It can be seen that the strongest diffraction intensity is the broad peak around $2\theta = 17$–$23°$ due to the substrate chitosan. In Fig. 7b the peaks at $2\theta = 11.5°$, 20.8°, 22.4°, 29°, 32°, 34°, and 44° are ascribed to the diffraction of $CaSO_4 \cdot 2H_2O$ (gypsum).

In addition, Fig. 6 shows the fine powder XRD patterns of the grafted chitosan after the crystallization assays using CHI-g-PAAM (HMW, KPS 2×10^{-2} M). It can clearly seen the peaks at $2\theta = 11.6°$, 20.7°, 20.7°, 23.5°, 29.1°, 31.1°, 33.3°, and 43.5°, confirming the occurrence of $CaSO_4 \cdot 2H_2O$.

In the case of SEM observations of calcium carbonate crystals formed on a CHI-g-PAA surface (LMW, KPS 1×10^{-2} M), Figs. 4e and 4f showed that they present a novel and attractive donut-like form. Even at high magnification, no sign of defined crystal structure was evident. This was the first indication that this $CaCO_3$ form might correspond to an amorphous phase. Therefore we obtained a powder X-ray diffraction analysis of this sample (Fig. 8).

Fig. 8a shows the XRD patterns of the chitosan and Fig. 8b the XRD pattern of donut $CaCO_3$ particles grown on the grafted CHI-g-PAA (LMW, KPS 1×10^{-2} M). This pattern is practically identical to that of the ungrafted chitosan, without the presence of peaks attributable to a crystalline phase what could indicate the presence of an amorphous $CaCO_3$ phase. Transient stabilization of amorphous $CaCO_3$ phase by polycarboxylate additives (acrylic acid/maleic acid copolymer) as a first stage of the precipitation was confirmed by Rieger et al. using time-resolved X-ray scattering experiments [28]. Table 4 show a summary of the different crystal forms by SEM analysis.

4. Summary

The mineralization of calcium salts done in the presence of chitosan of high (HMW) or low molecular weight (LMW), grafted in each case with either PAAM or PAA with two concentrations of KPS, resulted in particles with a variety of crystalline structures and morphologies.

A dramatic influence of the particular composition of grafted chitosan, used as a structure-directing substrate, on the crystalline habit of calcium salts was found. The different active groups present in the grafted chains interact differently with the individual growing planes of the crystals. In experiments done with CHI grafted with polyacrylamide, it was found that rosette shaped $CaSO_4$ crystals are formed. This indicates that, in spite of the exhaustive extraction of the grafted copolymers with water, sulfate groups coming from the KPS remains in the product, probably associated with the grafted polyacrylamide chains. In the case of crystallization on CHI-g-PAA films small spheres or donuts-like shaped $CaCO_3$ particles were selectively formed. Further investigation in the direction of the mechanism of the $CaSO_4$ rosette crystals growing, influence of acidic functional group stereochemistry and crystal kinetic analysis are under progress to achieve the understanding of heterogeneous crystallization on grafted chitosans. Regarding the mechanism of the $CaSO_4$ crystals, we suggest that crystal growth could take place inside the grafted CHI-g-PAAM films with subsequent escalation and grown up to the surface. This kind of mechanism was recently reported for some superstructure of $CaCO_3$ particles [29,30].

Acknowledgments

This research was supported by Project FONDAP 11980002 granted by the Chilean Council for Science and Technology (CONICYT).

References

[1] S. Mann, G.A. Ozin, Nature 382 (1996) 313.
[2] H.A. Lowenstam, S. Weiner, On Biomineralization, Oxford Univ. Press, Oxford, 1989.
[3] J.L. Arias, A. Neira-Carrillo, J.I. Arias, C. Escobar, M. Bodero, M. David, M.S. Fernández, J. Mater. Chem. 14 (2004) 2154.
[4] S. Mann, Biomineralization, Oxford Univ. Press, Oxford, 2001.
[5] J.L. Arias, M.S. Fernandez, Mater. Charact. 50 (2003) 189.
[6] H.C.W. Skinner, A.H. Jahren, Treatise Geochem. 8 (2003) 117.
[7] R. Sheikholeslami, M. Ng, Ind. Eng. Chem. Res. 40 (2001) 3570.
[8] F. Manoli, S. Koutsopoulus, E. Dalas, J. Cryst. Growth 189 (1997) 116.
[9] T. Kato, T. Suzuki, T. Irie, Chem. Lett. 29 (2000) 186.
[10] N. Hosoda, T. Kato, Chem. Mater. 13 (2001) 688.
[11] P. Liang, Y. Zhao, Q. Shen, D. Wang, D. Xu, J. Cryst. Growth 261 (2004) 571.
[12] O. Grassmann, G. Müller, P. Löbmann, Chem. Mater. 14 (2004) 4530.
[13] S. Zhang, K.E. Gonsalves, J. Appl. Polym. Sci. 56 (1995) 687.
[14] S. Zhang, K.E. Gonsalves, Langmuir 14 (1998) 6761.
[15] A. Sugawara, T. Kato, Chem. Commun. 6 (2000) 487.
[16] T. Kato, Adv. Mater. 12 (2000) 1543.
[17] T. Kato, T. Suzuki, T. Amamiya, T. Irie, Supramol. Sci. 5 (1998) 411.
[18] K. Kurita, Prog. Polym. Sci. 26 (2001) 1921.
[19] E. Khor, L.Y. Lim, Biomaterials 24 (2003) 2339.
[20] M. Yazdani-Pedram, A. Lagos, J. Retuert, J.M.S. Pure, Appl. Chem. A 32 (5) (1995) 1037.
[21] M. Yazdani-Pedram, J. Retuert, J. Appl. Polym. Sci. 63 (1997) 1321.
[22] M. Yazdani-Pedram, A. Lagos, J. Retuert, Polym. Bull. 48 (2002) 93.
[23] D. Volkmer, M. Fricke, C. Agena, J. Mattay, J. Mater. Chem. 14 (2004) 2249.
[24] J.M. Domínguez-Vera, J. Gautron, J.M. García-Ruiz, Y. Nys, Poultry Sci. 79 (1999) 901.
[25] J.I. Arias, J.P. Wiff, M.S. Fernandez, V. Fuenzalida, J.L. Arias, Mater. Res. Soc. Symp. Proc. 711 (2002) 243.
[26] S. Durmaz, O. Okay, Polymer 41 (2000) 3693.
[27] O. Grassmann, P. Löbmann, Chem. Eur. J. 9 (2003) 1310.
[28] J. Rieger, J. Thieme, C. Schmidt, Langmuir 16 (2000) 8300.
[29] J. Rudloff, H. Cölfen, Langmuir 20 (2004) 991.
[30] S.-H. Yu, H. Cölfen, J. Mater. Chem. 14 (2004) 2124.